

## Polarity Switching and Transient Responses in Single Nanotube Nanofluidic Transistors

Rong Fan,<sup>1</sup> Min Yue,<sup>2</sup> Rohit Karnik,<sup>2</sup> Arun Majumdar,<sup>2,3</sup> and Peidong Yang<sup>1,3,\*</sup>

<sup>1</sup>Department of Chemistry, University of California, Berkeley, California 94720, USA

<sup>2</sup>Department of Mechanical Engineering, University of California, Berkeley, California 94720, USA

<sup>3</sup>Materials Sciences Division, Lawrence Berkeley National Laboratory, Berkeley, California 94720, USA

(Received 1 May 2005; published 19 August 2005)

We report the integration of inorganic nanotubes into metal-oxide-solution field effect transistors (FETs) which exhibit rapid field effect modulation of ionic conductance. Surface functionalization, analogous to doping in semiconductors, can switch the nanofluidic transistors from *p*-type to *ambipolar* and *n*-type field effect transistors. Transient study reveals the kinetics of field effect modulation is controlled by ion-exchange step. Nanofluidic FETs have potential implications in subfemtoliter analytical technology and large-scale nanofluidic integration.

DOI: 10.1103/PhysRevLett.95.086607

PACS numbers: 85.30.Tv, 66.10.Ed, 82.65.+r

The ability to manipulate charge carriers (electrons and holes) in metal-oxide-semiconductor field effect transistors (MOSFETs) has revolutionized how information is processed and stored, and created the modern digital age. Analogous to MOSFETs, introducing field effect modulation in micro or nanofluidic systems in a three-terminal device would enable the manipulation of ionic and molecular species at a similar level and even logic operation. Because of strong Debye screening in aqueous solutions [1], field effect modulation of ion transport arises only in systems whose dimensions are comparable to the critical Debye Length, i.e., nanofluidic channels [2].

Nanofluidics has already attracted remarkable attention for ultrasensitive or even single molecule level detection and biological activity study [3]. For instance, membrane channel proteins and artificial solid state nanopores were utilized for single molecule sensing, configuration study, and DNA sequencing [4,5]. These nanochannel/nanopore devices usually passively transport ionic species, similar to electrical resistors. Analogous to unipolar MOSFETs, introducing external electrical field to modulate ionic conductivity would promote nanofluidics to a higher level of controllability or even logic. It is also notable that the single conical nanopore has been reported to exhibit active rectified ion transport in a two-terminal device configuration [6]. Single nanochannel studies have shown that the surface charge governs the ionic transport and induces the formation of unipolar solutions as in unipolar MOSFETs [7,8]. Metal nanotubule membranes exhibited selective ion flux upon electrochemically tuning surface charges [9]. These results suggest feasibility of developing single nanotube ionic field effect transistors. Here, we report a rapid field effect control of electrical conductance in single nanotube nanofluidic transistors, their polarity switching upon surface functionalization and the transient responses upon field effect control.

Chemically synthesized silica nanotubes with high aspect ratio, excellent uniformity and surface smoothness [10] were integrated into single nanotube nanofluidic tran-

sistors by interfacing with two microfluidic channels [Fig. 1(a)] [8]. The devices include lithographically defined gate electrodes, deep etched source-drain microfluidic channels, and a polydimethylsiloxane (PDMS) cover [Fig. 1(b)]. The concentration dependence of ionic conductance deviates from bulk behavior when  $[KCl] < 10$  mM, which indeed confirms the formation of unipolar ion transport [7,8], and lays the foundation for further field effect modulation. When applying gate voltages ( $V_g$ ), the electrical conductance of KCl solution ( $\leq 1$  mM) decreases with changing  $V_g$  from negative to positive, a characteristic of *p*-type transistors.

Similar to field effect modulation in metal-oxide-semiconductor (MOS) systems [11], gate voltages shift the electrostatic potential distribution inside the nanotubes (Fig. 2 top inset). In the solution, an electrical double layer (EDL) forms to screen the surface potential. The EDL consists of the inner compact layer (Stern layer) and the outer diffuse layer [12]. In a fluid medium sufficiently larger than the thickness of the diffuse layer, the electrostatic potential decays from the effective surface potential ( $\zeta$  potential) to zero. When the solution is confined in a nanotube whose dimension is comparable to or smaller than the diffuse layer, the electrical potential remains non-

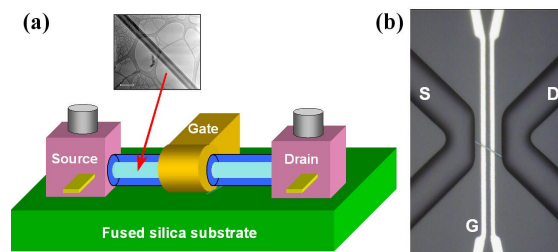


FIG. 1 (color online). Single nanotube nanofluidic transistors. (a) Schematic of MOSolFETs. Inset is a TEM image of a chemically synthesized silica nanotube. Scale bar is 100 nm. (b) An optical image showing the device structure. The nanotubes are  $\sim 40$ – $50$  nm in inner diameter and  $\sim 15$   $\mu$ m in length.

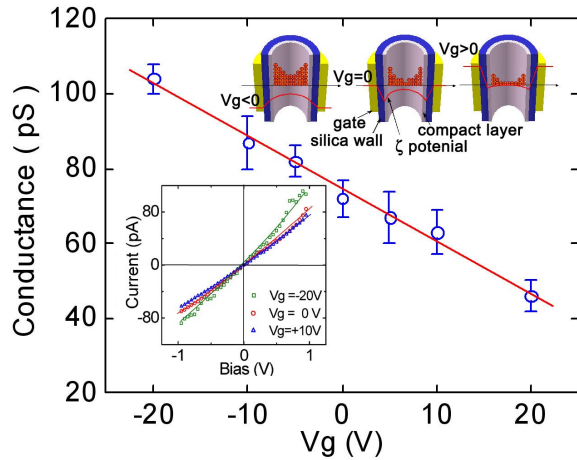


FIG. 2 (color online). Ionic conductance vs gate voltage. Error bars are  $1\sigma$ . Top inset schematically shows field effect modulation of electrical potential diagram in MOSFETs. Bottom inset shows selected  $I/V$  curves. All data are obtained after zero shift correction.

zero even in the middle of nanotubes. In the case of silica nanotubes having negative surface charges, cations are majority carriers and the resulting transistors are  $p$  FETs. Negative  $V_g$  enhances cation concentration while positive  $V_g$  depletes cations. This simple scheme explains qualitatively how field effect control works in nanofluidic systems.

Analogous to semiconductors, we also wish to tune the “doping level” and change inherent carrier concentrations or type, and systematically study field effect operation in nanofluidic transistors. It is now clear that the inherent carrier concentration in nanofluidic transistors is controlled by the inner surface potential and charge density. In this regard, surface modification is expected to have a similar consequence to nanofluidic transistors as doping in semiconductors to MOSFETs. Reduced doping level is generally associated with pronounced field effect modulation in

semiconductors [13]. We now turn to the impact of surface modification on the field effect for our metal-oxide-solution field effect transistors (MOSofFETs).

Aminosilane chemistry was used to modify the inner surfaces of silica nanotubes in order to change the surface potential and the charge density or even switch channel polarity. Right before PDMS cover bonding, the nanotube was treated with 3-amino-propyltriethoxysilane (APTES) [Fig. 3(a)] while the transistor characteristics were monitored over the surface functionalization duration [14]. It was found that 1 day of APTES functionalization did not change polarity (still  $p$ -type behavior), but led to greatly reduced ionic conductance and more pronounced gating effect [Fig. 3(b)]. The ionic conductance exhibits much more profound and fairly stable field effect modulation, and a relatively lower noise level compared to as-made devices [Figs. 3(c) and 3(d) top].

Interestingly, two days of APTES functionalization resulted in ambipolar transport behavior [Fig. 3(e) top]. Negative gate voltage increased conductance significantly due to the enhancement of cations as in  $p$  FETs. A positive  $V_g$  of 5 V slightly decreased conductance due to the depletion of cations, but when  $V_g$  was above 5 V, ionic conductance again increased as one would expect for  $n$  FETs. We attribute this observation to surface charge reversal after passing the ambipolar point. Under large positive  $V_g$  ( $> 5$  V), anions became the majority carrier which resulted in an  $n$  FET. In semiconductor systems, small band gap materials tend to exhibit more profound ambipolar behavior [15]. Nanofluidic transistors, in which both cation and anion densities are associated with the same electrical potential level, are essentially gapless transport systems. Consequently, ambipolar behavior would be expected once the inherent carrier concentration falls into suitable low concentration regime.

The polarity of the nanotube ionic transistors can be completely reversed after long time surface modification. Four days of APTES treatment converted as-made  $p$  FETs

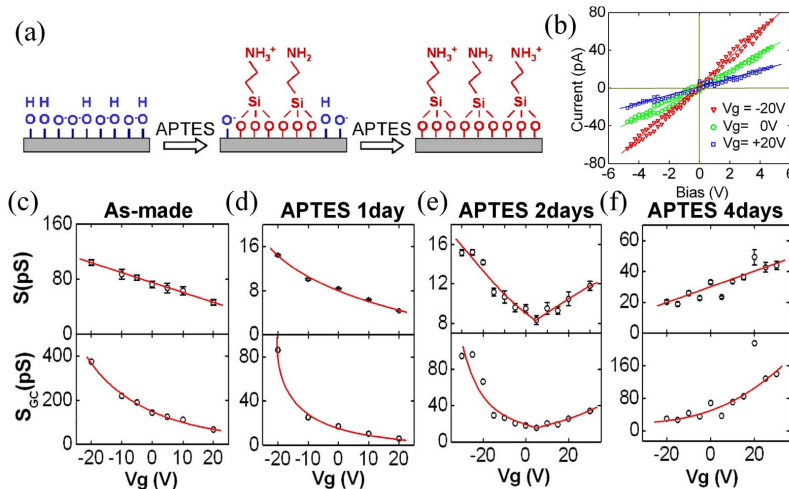


FIG. 3 (color online). Doping control and polarity reversal. (a) Schematic of nanotube inner surface modification with APTES. (b) Selected  $I/V$  curves for the nanofluidic transistor after 1 day of APTES treatment. (c-f) Measured ionic conductances ( $S$ ) and the effective conductance at gate controlled regions ( $S_{GC}$ ) vs gate voltages for as-made, and functionalized MOSofFETs.

into  $n$  FETs [Fig. 3(f) top]. Within the experimental range of  $V_g$ , conductance increased monotonously with increasing  $V_g$ . For all  $n$ -FET devices, the conductance at zero  $V_g$  is always lower than that for as-made nanotube devices, but greater than that for the devices after 1 or 2 days of APTES treatment. This polarity switching is highly reproducible in various devices and by using different APTES concentrations.

In our nanofluidic transistors, the regions that were not covered by gate electrodes resulted in series resistance, as shown in Fig. 1(b) [2]. The effective conductance under gate electrode control ( $S_{GR}$ ) was obtained for both the as-made and all the functionalized transistors by subtracting series resistances [Figs. 3(c)–3(f) bottom].  $S_{GR}$  exhibits up to tenfold field effect modulation in our experiments. The region of a nanotube underneath a single gate electrode ( $\sim 4 \mu\text{m}$  wide) is as small as  $\sim 8$  attoliter. The rapid and reversible modulation of ionic concentration or even locally switching the carrier polarity in such a small volume might represent the finest control of ion distribution in fluidic systems.

Field effect modulation in MOS systems relies on capacitive coupling between metallic gates and semiconductors. Capacitive coupling also plays a key role in our metal-oxide-solution (MOSol) systems. A three-capacitor model was proposed by van den Berg *et al.* to semiquantitatively explain the relationship between gate voltage and  $\zeta$  potential change in their flow FETs [16]. As shown in Fig. 4(a) inset,  $C_{ox}$ ,  $C_{ST}$  and  $C_{DL}$  represent the capacitances of the silica nanotube wall, the compact layer, and the diffuse layer, respectively. Since the compact layer is very thin ( $< 1 \text{ nm}$ ) and has a large dielectric constant ( $\sim 80$ ) as in aqueous solutions,  $C_{ST}$  is very large and therefore negligible when connected in series with  $C_{ox}$  and  $C_{DL}$ . So the  $\zeta$  potential change ( $\Delta\zeta$ ) can be calculated by  $\Delta\zeta = (C_{ox}/C_{DL})V_g$ . This model predicts a linear relation between  $\zeta$  potential and gate voltages.  $\Delta\zeta$  could be as large as 200 mV at  $V_g = 20 \text{ V}$ . In order to find out the experimental values of  $\zeta$  potential and surface charge density, Possion-

Boltzmann equations were used to numerically solve for the potential and ion distributions across the nanotube as a function of  $\zeta$  potential [1]. Integration of the anion and cation densities in the whole nanotube yields the conductance enhancement factor as a function of  $\zeta$  potential and surface charge density [8].

By comparing theoretical and experimental conductance enhancement factors—effective conductance ( $S_{GR}$ ) over the conductance of bulk solution if confined in the same volume, the corresponding  $\zeta$  potential and surface charge density were estimated as shown in Figs. 4(a) and 4(b). It turns out  $\zeta$  potential changes with  $V_g$  almost linearly, in agreement with the prediction of the three-capacitor model. In contrast to its prediction that field effect modulation of  $\zeta$  potential is concentration independent, the  $\zeta$  potential modulation is greater in low inherent  $\zeta$  potential devices (low “doping” level). The observed  $\zeta$  potential changes between  $V_g = -20 \text{ V}$  and  $+20 \text{ V}$  range from  $\sim 1$  to  $5.5k_B T/e$ , which is smaller than the theoretical value 200 mV ( $7.8k_B T/e$ ). This discrepancy might be due to the effective distance of the diffuse layer which is not simply equal to Debye length, but varies with surface potential.

Effective surface charge densities vs  $V_g$  are shown in Fig. 4(b). As-made  $p$ -type nanofluidic transistors exhibit fourfold field effect modulation of surface charge density. The “APTES 1 day” device has greatly reduced inherent surface charge density, and exhibits greater field effect modulation ( $\sim$ tenfold). The  $n$ -type FET exhibits fivefold field effect modulation and lower inherent surface charge density (at  $V_g = 0 \text{ V}$ ) compared to as-made  $p$ -type FETs. This difference might arise from the different deprotonation or protonation constants of the hydroxyl group and the amino group. The ambipolar device exhibits a surface charge density switch from negative to positive when  $V_g$  is greater than 5 V. Theoretically, the surface charge density can be reduced down to zero to completely turn off the fluidic transistor. The experimental data shows large OFF state conductance and charge density, possibly due to the existence of parasitic conductance at the bottom side of

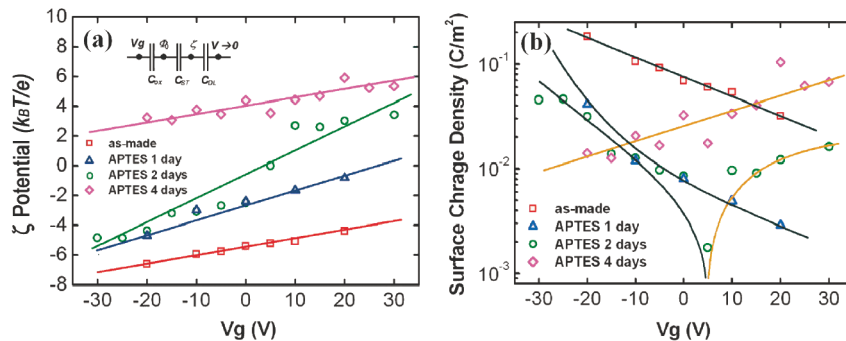


FIG. 4 (color). Field effect modulation of  $\zeta$  potentials (a) and surface charge densities (b) for as-made and all functionalized devices. Inset in (a) shows the three-capacitor model. The solid lines are drawn as a guide for the eyes only. The black lines represent negative surface charges, while orange lines represent positive surface charges. For the surface charge modulation of “APTES 2 days,”  $V_g = 5 \text{ V}$  is defined as the ambipolar point where surface charge density is zero.

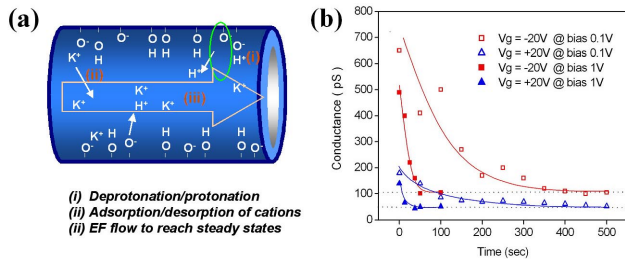


FIG. 5 (color online). Transient phenomena for field effect control. (a) Schematic of the surface chemical reactions and electrokinetic effect involved in field effect modulation. (b) The transient responses of ionic conductance when turning on the gate voltages. Dashed lines represent the steady states.

nanotubes, which is not wrapped by metallic gate electrode and does not necessarily respond to the applied gate voltage. Our study provides the first opportunity to assess these electrostatics theories in nanoscale and have significance in improving fundamental understanding of nanoscale physics in solution systems.

Lastly, we have examined the kinetic process of field effect control in nanofluidic transistors. In a hydroxyl group terminated silica nanotube filled with KCl solution, once a gate voltage is applied, there are three basic kinetic processes [Fig. 5(a)]: (i) deprotonation or protonation in response to the external electrical field, (ii) adsorption or desorption of counter ions in the compact layer, (iii) ion exchanges between the transiently generated counter ions and bulk solution in microfluidic channels leading to a steady state of ion distribution. The experimental data shows that the ionic conductance jumps up once gate voltages are turned on due to transient accumulation of the ions induced by surface reaction (i) and/or (ii). It decays gradually down to steady states (dashed line). At the same gate voltages, high bias sweeping leads to a rapid decay (relaxation time  $< 60$  sec at 1 V) while low bias gives a slow decay (relaxation time  $\sim 250$  sec at 0.1 V). Such a strong bias dependence has been observed for both negative and positive  $V_g$ 's. When the bias is swept between  $\pm 5$  V, the conductance reaches a steady state immediately in single  $I/V$  scan (10–20 sec). On the other hand, it has been found that at the same bias, different gate voltages did not result in much different transient responses. Hence, the ion-exchange step is believed to control the kinetics of field effect modulation in nanofluidic transistors. Further reducing the nanotube dimension and increasing bias should lead to faster field effect operation.

This work was supported by National Cancer Institute and the Basic Energy Sciences, Department of Energy.

\*Electronic address: p\_yang@berkeley.edu

- [1] J. Israelachvili, *Intermolecular and Surface Forces* (Academic Press, London, 2003), 2nd ed..
- [2] H. Daiguji, P.D. Yang, and A. Majumdar, *Nano Lett.* **4**, 137 (2004).
- [3] S.W.P. Turner, M. Cabodi, and H.G. Craighead, *Phys. Rev. Lett.* **88**, 128103 (2002).
- [4] J.J. Kasianowicz, E. Brandin, D. Brandon, and D.W. Deamer, *Proc. Natl. Acad. Sci. U.S.A.* **93**, 13770 (1996); S. Howorka, S. Cheley, and H. Bayley, *Nat. Biotechnol.* **19**, 636 (2001); D.W. Deamer and M. Akeson, *Trends Biotechnol.* **18**, 147 (2000).
- [5] J.L. Li *et al.*, *Nat. Mater.* **2**, 611 (2003); A.J. Storm *et al.*, *Nano Lett.* **5**, 1193 (2005); O.A. Saleh and L.L. Sohn, *Nano Lett.* **3**, 37 (2003); A. Mara *et al.*, *Nano Lett.* **4**, 497 (2004).
- [6] Z. Siwy *et al.*, *Appl. Phys. A: Mater. Sci. Process.* **76**, 781 (2003); Z. Siwy and A. Fulinski, *Phys. Rev. Lett.* **89**, 198103 (2002); Z. Siwy, I.D. Kosinska, A. Fulinski, and C.R. Martin, *Phys. Rev. Lett.* **94**, 048102 (2005).
- [7] P.D. Yang, in *Proceedings of the American Chemical Society 227th National Meeting, Anaheim, CA, 2004 (Part 2)* (American Chemical Society, Washington, DC, 2004) Abstract No. 497; D. Stein, M. Kruithof, and C. Dekker, *Phys. Rev. Lett.* **93**, 035901 (2004); R. Karnik *et al.*, *Nano Lett.* **5**, 943 (2005).
- [8] See EPAPS Document No. E-PRLTAO-95-054534 for details of the device fabrication, the scanning electron microscopy characterization, the theoretical and experimental data about the unipolar ionic environment and transport, and the mathematical model to calculate  $\zeta$  potentials and surface charge densities using Poisson-Boltzmann equations. This document can be reached via a direct link in the online article's HTML reference section or via the EPAPS homepage (<http://www.aip.org/pubservs/epaps.html>).
- [9] M. Nishizawa, V.P. Menon, and C.R. Martin, *Science* **268**, 700 (1995); M.S. Kang and C.R. Martin, *Langmuir* **17**, 2753 (2001); T.C. Kuo, L.A. Sloan, J.V. Sweedler, and P.W. Bohr, *Langmuir* **17**, 6298 (2001).
- [10] R. Fan *et al.*, *J. Am. Chem. Soc.* **125**, 5254 (2003).
- [11] R.F. Pierret, *Semiconductor Device Fundamentals* (Addison-Wesley, New York, 1996).
- [12] R.J. Hunter, *Foundations of Colloid Science* (Oxford University Press, New York, 2001), 2nd ed..
- [13] Y. Cui, X.F. Duan, J.T. Hu, and C.M. Lieber, *J. Phys. Chem. B* **104**, 5213 (2000).
- [14] T. Nakagawa *et al.*, *J. Biotechnol.* **116**, 105 (2005).
- [15] J.A. Misewich *et al.*, *Science* **300**, 783 (2003); T. Shimada *et al.*, *Appl. Phys. Lett.* **84**, 2412 (2004).
- [16] R.B. Schasfoort, S. Schlautmann, J. Hendrikse, and A. van den Berg, *Science* **286**, 942 (1999).